REY-Th-U Solute Dynamics in the Critical Zone: Combined Influence of Chemical Weathering, Atmospheric Deposit Leaching, and Vegetation Cycling (Mule Hole Watershed, South India)

Jean Braun, Jean Riotte, Shrema Battacharya, Aurélie Violette, Jonathan Prunier, Vincent Bouvier, Frédéric Candaudap, Jean-Christophe Maréchal, Laurent Ruiz, Smruthi Rekha Panda, et al.

AGU PUBLICATIONS

Geochemistry, Geophysics, Geosystems

RESEARCH ARTICLE
10.1002/2017GC007158

Key Points:
- Source of solute rare earths, thorium, and uranium in the Mule Hole tropical watershed has two main origins: heavy accessory bearing minerals and atmospheric dusts
- Rare earths and thorium, mainly from atmospheric dust leaching origin, are significantly recycled by vegetation and exported by overland flow as organic complexes
- Solute export by groundwater is much more significant for uranium than for rare earths and thorium, which transfer is limited by precipitation of secondary phosphates and oxides

Correspondence to:
J.-J. Braun,
jean-jacques.braun@ird.fr

Citation:
Braun, J.-J., Riotte, J., Battacharya, S., Violette, A., Prunier, J., Bouvier, V., . . . Subramanian, S. (2017). REY-Th-U solute dynamics in the critical zone: Combined influence of chemical weathering, atmospheric deposit leaching, and vegetation cycling (mule hole watershed, South India). *Geochemistry, Geophysics, Geosystems*, *18*, 4409–4425. https://doi.org/10.1002/2017GC007158

Received 31 JUL 2017
Accepted 11 NOV 2017
Accepted article online 15 NOV 2017
Published online 11 DEC 2017

REY-Th-U Solute Dynamics in the Critical Zone: Combined Influence of Chemical Weathering, Atmospheric Deposit Leaching, and Vegetation Cycling (Mule Hole Watershed, South India)

Jean-Jacques Braun[1,2], Jean Riotte[1,3], Shrema Battacharya[4,5], Aurélie Violette[1], Jonathan Prunier[1], Vincent Bouvier[1], Frédéric Candaudap[1], Jean-Christophe Maréchal[6], Laurent Ruiz[3,7], Smruthi Rekha Panda[5], and S. Subramanian[3,8]

[1]Géosciences Environnement Toulouse, Université de Toulouse, CNRS, IRD, Toulouse, France, [2]Institut de Recherches Géologiques et Minières/Centre de Recherches Hydrologiques, Yaoundé, Cameroon, [3]IISc-IRD Joint International Laboratory, IISc, Indo-French Cell for Water Sciences, Bangalore, Karnataka, India, [4]Physical Research Laboratory, Ahmedabad, Gujarat, India, [5]Center for Earth Science, IISc, Bangalore, Karnataka, India, [6]BRGM-Service Eau, Montpellier, France, [7]INRA Agrocampus Rennes, UMR, Sol-Agronomie-Spatialisation, Rennes, France, [8]Materials Engineering Department, IISc, Bangalore, Karnataka, India

Abstract The source and proportion of REY, Th, and U exported by groundwater and by the ephemeral stream along with the elemental proportions passing through vegetation have been assessed in the subhumid tropical forested CZO of Mule Hole, Southern India. The study relies on a pluriannual hydrogeochemical monitoring combined with a hydrological model. The significant difference between the soil input (SI) and output (SO) solute fluxes (mmol/km^2/yr) of LREE (SI-SO = 13,250-1,500), HREE (1,930-235), Th (64-12), and U (63-25) indicates a strong uptake by roots carried by canopy and forest floor processes. The contribution of atmospheric dust leaching can reach about 60% of LREE and 80% of HREE. At the watershed scale, the U solute flux exported by groundwater (180 mmol/km^2/yr) mainly originates from the breakdown of primary U-bearing accessory minerals and dominates by a factor of 25 the stream flux. The precipitation of authigenic U-bearing phases and adsorption onto Fe-oxides and oxyhydroxides play a significant role for limiting the U mobility. In the groundwater, the plagioclase chemical weathering is efficiently traced by the positive Eu-anomaly. The very low (REY) to nil (Th) contents are explained by the precipitation of authigenic phases. In the stream flow, dominated by the overland flow (87% of the yearly stream flow), the solute exports (in mmol/km^2/yr) of REY (1,080 for LREE and 160 for HREE) and of Th (14) dominate those by groundwater. Their mobility is enhanced by chelation with organic ligands produced by forest floor and canopy processes.

1. Introduction

The high field strength elements (HFSE) lanthanides (REE + Y = REY) and actinides (U, Th) are useful as geochemical tracers in studying terrestrial weathering and sediment transport. The solute dynamics of REY-Th-U are driven in first order by surface and groundwater fluxes (Lin, 2010; Ribera et al., 1996; Vázquez-Ortega et al., 2015). These elements thus participate in the exchanges with mineral phases and soil organic matter (SOM) and the plant-nutrient cycle (Derry & Chadwick, 2007; Stille et al., 2006). Numerous studies reported the behavior of REY-Th-U during chemical weathering of silicate rocks and solute/colloidal exports through river systems (Chabaux et al., 2003; Laveuf & Cornu, 2009 and references therein), but little is known about the contribution of atmospheric processes and vegetation cycling to the REY-Th-U export by surface and groundwater.

The solute inputs of REY-Th-U within the Critical Zone engine of pristine forested watersheds developed on silicate rocks have two sources: Chemical weathering of heavy accessory minerals, primarily bearing REY-Th-U phases, and leaching of atmospheric aerosol deposits. After being mobilized, these HFSE can be involved into the hydrobiogeochemical cycle, which encompasses processes as diverse as precipitation-dissolution of authigenic phases, oxidation-reduction (e.g., for Ce(III)/Ce(IV) and U(IV)/U(VI)), adsorption-desorption,

occlusion, and chelation (Davranche et al., 2011; Dupré et al., 1999; Gruau et al., 2004; Grybos et al., 2007; Gueniot et al., 1988a, 1988b; Jerden et al., 2003; Langmuir & Herman, 1980; Pourret et al., 2007a, 2007b; Steinmann & Stille, 2008; Viers et al., 1997). REY-Th-U are also mobilized by the plant-nutrient cycle, which implies uptake by roots, immobilization in hypogenous and *epigenous* biomass and partial elemental release by leaf excretion and/or litter fall and decay (Brioschi et al., 2013; Ribera et al., 1996; Sheppard & Evenden, 1988; Stille et al., 2006; Tyler, 2004).

In their seminal works on atmosphere-plant-soil, REE fractionation carried out on the temperate Strengbach CZO, Aubert et al. (2006) used Sr-Nd isotopes and observed that Sr and REE of stream water and trees mainly originate from preferential breakdown of apatite during weathering and that the preferential uptake of those LREE by vegetation amplifies the depletion of LREE in the catchment surface runoff. Vegetation could be a significant factor controlling LREE in rivers (Stille et al., 2006). By comparing the Strengbach brook REE signature with that of other rivers worldwide from low to high latitudes, the authors pointed out that the LREE depletion tends to disappear at higher latitudes due to either disappearance of vegetation or due to superposition of both, the disappearance of vegetation and the increasing importance of LREE enrichment of the organic-rich colloidal phases. A further study suggests that the evolution of the REE in the soil solutions is due to the following processes taking place above 50 cm depth: (i) precipitation of LREE-rich phosphate minerals like rhabdophane, (ii) diminution of the formation of organic dissolved or colloidal phases in association with Fe-Mn and Al oxyhydroxides, and (iii) preferential LREE uptake by vegetation (Stille et al., 2009). Solute residence time in the regolith is a key factor of REE contents and fractionation (Aubert et al., 2002), where water transfer from thin soil cover to river is very fast and stream water REE mainly originates from atmospheric inputs. Throughfall is slightly more enriched especially in LREE than filtered rainwater may be due to the leaching of atmospheric particles deposited on the canopy and also due to the leaf excretion. Nonetheless, little is known about the solute behavior of REE and U-Th in the Tropics at the water-soil-plant-atmosphere scale. Thus, the present paper will address the combined impact of chemical weathering, vegetation cycling, and atmospheric deposit leaching on the export of REY-Th-U by groundwater and stream in the tropical forested Mule Hole CZO, Southern India. The integrated investigations of this extensively studied experimental watershed aim at quantitatively predicting the Critical Zone structure and functioning, focusing on the pathways and the fluxes of water, solutes, and sediments using hydrological and geochemical tracers (Braun et al., 1998, 2009; Maréchal et al., 2009, 2011; Riotte et al., 2014a; Ruiz et al., 2010; Violette et al., 2010a).

Recently, in companion papers (Riotte et al., 2014a, 2014b), a hydrological model-based approach was combined with the concentrations of the major soluble elements (Na, Mg, K, Ca, and silica) at both soil profile and watershed scales to ascertain the elemental proportion passing through vegetation prior to being exported in the stream. The approach combining geochemical monitoring and accurate knowledge of the watershed hydrological budget provided a detailed understanding of several effects of vegetation on the stream fluxes, (i) evapotranspiration (limiting), (ii) vertical transfer through vegetation from vadose zone to ground surface (enhancing), and (iii) redistribution by canopy leaching and litter decay.

Keeping a comparable approach, we have used the same hydrological model to assess the solute dynamics of REY-Th-U through the ecosystem reservoirs (atmosphere-soil-plant system) and the export by stream and groundwater. The investigations have been carried out with the HFSE composition of vegetation and atmospheric dry deposits and the solute chemistry of water reservoirs (rainfall, throughfall, overland flow, soil pore, groundwater, and stream).

2. Settings

The Mule Hole CZO was established in 2003 as part of the Environmental Observatory BVET (http://bvet.obs-mip.fr/fr; Riotte et al., 2014a) belonging to the French "Drainage Basins Network" (Réseau des Bassins Versants, RBV; http://rnbv.ipgp.fr/). This 410 ha watershed is located 11°72N and 76°42E in the subhumid part of the climatic gradient of the Kabini river basin in the Southwest part of Peninsular India (Figure 1).

The geochemistry of major elements and mineralogy of parent rocks, saprolite, and soil cover are detailed in Barbiéro et al. (2007), Braun et al. (2009), and Violette et al. (2010a). The dominant parent rock is Peninsular gneiss of the >2.8 Ga West Dharwar craton (Naqvi & Rogers, 1987) mainly composed of quartz, Na-plagioclase, and amphibole as major minerals, biotite, and epidote as minor minerals and sericite as

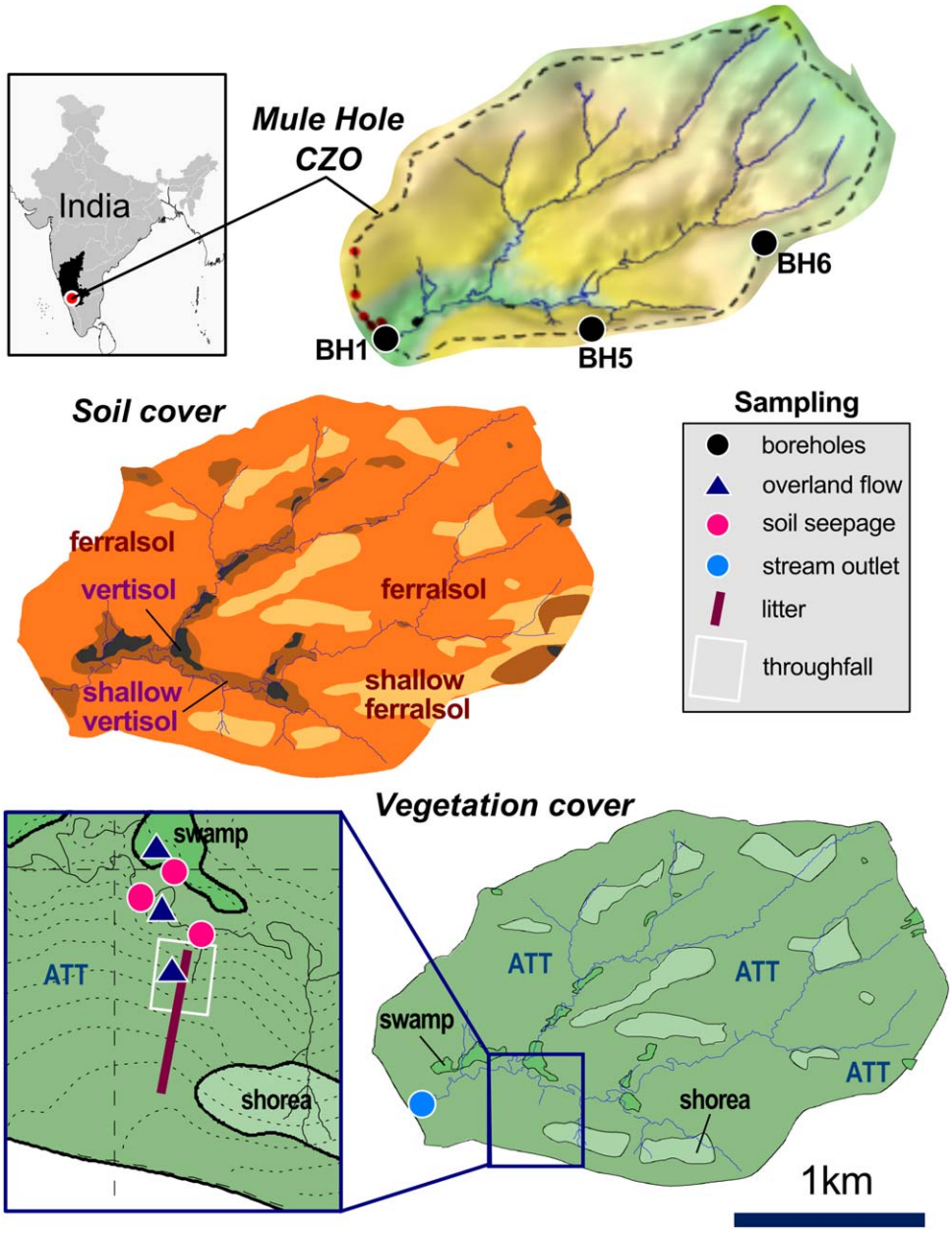

Figure 1. Soil and vegetation maps of the Mule Hole experimental watershed displaying the repartition of the main vegetation types (Medium green: ATT facies: *Anogeissus latifolia-Tectona grandis-Terminalia crenulata, Themeda triandra*; Dark green: swamp facies; Light green: Shorea facies), the repartition of the soil types and the sampling locations (modified from Riotte et al., 2014a).

alteration product of plagioclase. The gneiss exhibits pronounced hydrothermal alteration features, as illustrated by numerous hydrothermal seams rich in calcite, epidote, and albite. The alteration of the major phases is characterized by sericitization of plagioclase and chloritization of biotite by the pervasive fluids. Epidote is widespread. Occasionally, the gneiss is intermingled with less abundant amphibolites (Shadakshara Swamy et al., 1995). The amphibolite is composed of hornblende and anorthite as major mineral and calcite, epidote as minor minerals. At the watershed scale, the gneissic rocks cover 85% of the whole area and amphibolite the remaining 15%.

The saprolite has developed downward at the expense of the underlying fractured gneiss from which it does retain the structure and the fabric (i.e., isovolumetric weathering). It is immature and still contains significant amount of unweathered primary minerals such as Na-plagioclase. At the CZO scale, the average

regolith thickness is 17 m (Braun et al., 2009) of which 2 m of soil cover is present, on an average. The latter is composed of (i) ferralsols on the hill slopes (66% of the whole watershed area), (ii) vertisols either on flat valley bottoms on undifferentiated bedrocks and in the depressions on the crest line on amphibolite-rich bedrock (12% of the whole watershed area), and (iii) saprolite outcrop topped by thin ferralsol layers (22% of the whole watershed area; Barbiéro et al., 2007) (Figure 1). An assemblage of secondary clays and clay minerals dominated by kaolinite and goethite characterizes the ferralsol mineralogy. Residual crystals of quartz, sericite, and Na-plagioclase are preserved till the topsoil. The mineralogy of the gneiss-derived vertisols is dominated by smectite in the secondary clay assemblage upon kaolinite and kaolinite-smectite interstratified. In the amphibolite-derived vertisol, the mineralogy is dominated by smectite. The vertisol matrix contains pedogenic carbonates either tiny, disseminated or as pluricentimetric botryoidal nodules witness of dryer paleoclimatic conditions (Violette et al., 2010b).

The vegetation cover (Figure 1) is a dry deciduous forest, dominated by the "ATT facies," i.e., *Anogeissus latifolia* (*Roxb. ex DC. Wall. ex Guillem. & Perr.*), *Tectona grandis* (*Tectona grandis* L.f.), and *Terminalia crenulata* (*Terminalia crenulata* Roth.) for trees and *Themeda triandra* (*Themeda triandra Forssk.*; Elephant grass) for grass (Barbiéro et al., 2007; Riotte et al., 2014a; Violette et al., 2010b). This assemblage, developed on thick ferralsol and shallow vertisol, accounts for 70% of the watershed area. The remaining 30% consists in *Shorea* spec. trees, associated with well drained saprolite outcrops (topped by shallow ferralsol), and *Ceristoides* spec. trees typical from vertisol.

The Mule Hole SEW presents the contemporary weathering conditions for an immature weathering cover under subhumid climate successively fed by the South-West and North-East monsoon systems (6 months; Braun et al., 2009; Maréchal et al., 2009; Soumya et al., 2009; Ruiz et al., 2010). The Mean Annual Rainfall (MAR) over the last 30 years is 1,100 $\pm$ 250 mm/yr of which 10% is intercepted by the canopy. From the estimations given in Maréchal et al. (2009), long-term average evapotranspiration accounts for 80–90% of the annual rainfall, groundwater recharge for only 6 $\pm$ 2% and runoff for 8 $\pm$ 2%. This water balance indicates that vegetation limits both groundwater recharge and runoff and explains why groundwater and stream water are disconnected. The stream is then intermittent and the floods last from few hours to few days. Stream water originates from a mixing of (i) overland flow on ferralsol and vertisol from the vicinity of the thalweg and (ii) seepage flow (soil pore water) from the ferralsol during storm recession, at the end of the monsoon (when soils are waterlogged).

3. Materials and Methods

3.1. Chemistry of Leaf and Herbaceous Litters and Associated Atmospheric Dust Deposits

Leaf and herbaceous litters were collected during the dry seasons of the year 2009, 2010, and 2014 from the most widespread soil/vegetation configuration in the watershed, i.e., the ATT facies developed on ferralsol derived from gneiss. The detailed description of the sampling procedure is given in Riotte et al. (2014a) (Figure 1). A large dry sample (approx. 1 kg) of each major species, i.e., *A. latofolia*, *T. grandis*, *T. crenulata*, and *T. triandra* were carefully washed with deionized water to remove dusts and dried. Several grams of each sample were powdered with an agate mortar. An aliquot of 100 mg of powder was digested with HNO_3, HF, and H_2O_2 in a microwave oven Mars Express. Once dissolved, the samples were analyzed by ICPMS (Elan 6000, Geosciences Environnement Toulouse, France) using In and Re as internal standards and EPONDU-4 and SLRS-5 as external ones. The digestion procedure was checked for major elements using the reference material NIST 1515 (Apple leaves). The detection limit for REE-U-Th was about 2 ng g^{-1} of sample. Procedure blanks for these elements were found below the detection limit of ICPMS. The overall precision obtained for the concentration measurements above the quantification limit were about 10%.

The dry and wet atmospheric inputs encompass, in various proportions, diverse elemental sources as marine (cyclic salts), biogenic (e.g., biological emissions, biomass burning), geogenic (e.g., desert dust aerosols, volcanic ashes), and anthropogenic (industrial emissions). Analyzing the composition of the particles deposited on leaf and herb samples enables the assessment of the average composition of dry deposits. The particles were concentrated by centrifuging the leaf washing solution, before microwave digestion and ICPMS analysis as described above. Atmospheric dust deposition is a secondary but nontrivial source of minerals and nutrients to Earth's regoliths (Brimhall et al., 1988; Ferrier et al., 2011). The origin of geogenic dusts can be desert sand, barren soil surfaces or volcanic ashes. Particles can be incorporated in the soils

and can participate in the pedogenic processes. They can also be partly dissolved and participated in the nutrient cycle. In Peninsular India, the pathways for the wind direction, hence, the dust sources mainly originate from the Arabian Peninsula, Iran, Pakistan, and Thar Deserts (Goswami et al., 2014; Vinoj et al., 2014). The geogenic REY-Th-U signature of the particles is estimated with a linear regression model assuming that (i) 100% of Al of the atmospheric deposit concentrate is of geogenic origin and (ii) the end-member Al content of the dust aerosols ("pure" dust component) is similar to the Thar Desert dust composition (Al = 6.4 ± 1.2%; Ferrat et al., 2011; Yadav & Rajamani, 2004). The Thar Desert dust is composed of quartz (30%), illite/smectite (20%), albite (9%), muscovite (8%), chlorite (3%) calcite (10%), dolomite (8%), and actinolite (10%; Ferrat et al., 2011).

3.2. Water Chemistry of Wet Atmospheric Deposits, Throughfall, Overland Flow, Soil Pore Water, Stream, and Groundwater

The geochemical monitoring of the Mule Hole CZO, started in 2003, consists in collecting time series samples (i) at event level for flood and rainfall and (ii) monthly for groundwater. The Mule Hole outlet is equipped with an auto-sampler (ISCO®) collecting stream water samples every 60 or 90 min. Besides the monitoring, samples of throughfall deposits, overland flow, and soil pore waters seeping out from the stream banks were collected (Figure 1).

Wet open field atmospheric deposits were collected for each rainfall event, at the Mule Hole check-post, 1 km away from the outlet of the watershed. These samples were collected in 6 L polyethylene bags placed on a stand at 1.5 m height, i.e., in accordance with the international standards of rain collection (Lacaux et al., 1992). The solute chemistry of wet open field atmospheric deposits integrates most of the wet deposits but possibly only the soluble fraction of dry deposits.

In forested watersheds, the majority of incident rainfall reaches the ground from the canopies via throughfall (Bhat et al., 2011; Bruijnzeel, 1989, 1990; Carlyle-Moses et al., 2004). Hence, throughfall composition reflects processes occurring on the canopy as (i) interception, (ii) exudation of chemical elements by leaves and stems, (iii) direct uptake, and (iv) leaching of dry atmospheric deposits (Balestrini et al., 2007; Gandois et al., 2010, 2014; Lindberg et al., 1986; Lovett & Lindberg, 1984). Once the throughfalls reach the forest floor, they interact with the decaying litter blended with variable amount of atmospheric dusts. All these interactions control the chemical composition of the water that further infiltrates into the soil layers. The throughfall deposit samples ($n = 14$) were collected in September 2009 during a single rainfall event at Mule Hole under the main tree facies *A. latifolia-T. grandis-T. crenulata* (ATT), *T. triandra* along with few other tree species and shrubs, in order to address the species-related variability of rainfall interaction with canopy.

Table 1
Equations Used to Calculate the Fluxes Above Ground, Within the Soil, Within the Groundwater, and in the Stream of an Element j According to the Hydrological Model

	Water budget from Riotte et al. (2014a) (mm/yr)	Concentration (μmol/L)	Elemental flux (mol/ha/yr)	Equations
Above ground	P	$C^{VWM}_{j,wet\_deposits}$	$F_{j,wet\_atmospheric\_input}$	$\left(C^{VWM}_{j,wet\_deposits} \cdot P\right)/100$
	Q_{ground} = P-interception	$C^{VWM}_{j,throughfall}$	$F_{j,throughfall}$	$\left(C^{VWM}_{j,throughfall} \cdot Q_{ground}\right)/100$
	Q_{ground} = P-interception	$C^{VWM}_{j,overland\_flow}$	$F_{j,ground}$	$\left(C^{VWM}_{j,overland\_flow} \cdot Q_{ground}\right)/100$
			$F_{j,canopy\_interaction}$	$F_{j,throughfall} - F_{j,wet\_atmospheric\_input}$
			$F_{j,vegetation\_cycling}$	$F_{j,ground} - F_{j,wet\_atmospheric\_input}$
Soil	Q_{soil_input}		$F_{j,soil\_input}$	$\left(C^{VWM}_{j,overland\_flow} \cdot Q_{soil\_input}\right)/100$
	Q_{soil_output}	$C^{AV}_{j,seep\_flow}$	$F_{j,soil\_output}$	$\left(C^{AV}_{j,seep\_flow} \cdot Q_{soil\_output}\right)/100$
			$\Delta F_{j,soil}$	$F_{j,soil\_output} - F_{j,soil\_input}$
Groundwater	$Q_{recharge} = Q_{discharge}$	$C^{AV}_{j,groundwater}$	$F_{j,grdw\_discharge}$	$\left(C^{AV}_{j,groundwater} \cdot Q_{recharge}\right)/100$
Stream	Q_{stream}	$C^{VWM}_{j,streamwater}$	$F_{j,stream\_discharge}$	$\left(C^{VWM}_{j,streamwater} \cdot Q_{stream}\right)/100$

Note. Subscripts AV and VWM for average and volume weighted concentrations of element *j*.

AGU Geochemistry, Geophysics, Geosystems

10.1002/2017GC007158

Table 2

Contents of REY-Th-U, Zr, Ti and P, Sums and UCC-Normalized Ratios (Ce/Ce, Eu/Eu*, $(La/Sm)_N$, and $(Gd/Yb)_N$) of the Leaf and Herb Litter Along With Associated Atmospheric Deposits Which Is Recovered From Leaves and Herbs by Washing With Deionized Water*

Sample	Type	Concentration		La	Ce	Pr	Nd	Sm	Eu	Gd	Tb	Dy	Ho	Er	Tm	Yb	Lu	Y	∑LREE	∑HREE	∑REY	Th	U	Zr	Ti		P	Ce/Ce*	Eu/Eu*	La/Sm_N	Gd/Yb_N
T. grandis	Leaves		ng/g	689	426	59	223	54	15	53	9	36	6	6	2.5	12.7	3.6	155	1,465	129	1,749	42	1.6	137	BDL		425,548	0.51	1.07	1.94	1.80
A. latifolia	Leaves		ng/g	634	266	80	277	46	11	39	4	20	3	13	0.4	3.9	BDL	120	1,315	84	1,518	38	2.1	71	BDL		905,565	0.29	1.01	2.10	4.23
T. crenulata	Leaves		ng/g	1,120	298	172	633	108	26	89	10	40	7	23	1.3	9.5	BDL	254	2,358	181	2,793	25	2.3	68	BDL		1,126,855	0.17	1.07	1.58	4.02
Blend of leaves			ng/g	1,054	530	161	499	83	30	97	9	45	10	14	1.6	13.4	1.1	253	2,357	189	2,800	98	6.3	90	BDL		327,638	0.31	1.33	1.94	3.10
Average trees	av.			874	380	118	408	73	20	69	8	36	7	14	1.4	9.9	2.3	195	1,874	147	2,216	51	3.1	92	BDL		696,402	0.29	1.14	1.83	3.01
	±s			248	121	57	192	28	9	28	3	11	3	7	0.9	4.3	1.7	69	562	58	782	33	2.1	32			382,268	0.14	0.14	0.22	1.10
T. triandra	Elephant grass		ng/g	160	179	29	112	27	4	41	6	20	5	10	1.3	7.1	0.3	89	512	89	691	38	3.1	83	BDL		615,468	0.64	0.53	0.91	2.47
Atmospheric deposits	Elephant grass		ng/g	4,402	8,380	990	3,643	718	171	726	100	582	109	320	46	280	38	3,332	18,305	2,163	23,837	1,199	295								
Atmospheric deposits	Elephant grass		ng/g	463	851	103	364	73	18	71	10	54	11	35	4	28	4	323	1,872	212	2,411	82	28								
Atmospheric deposits	Leaves		ng/g	1,944	3,385	429	1,539	306	69	308	41	237	45	130	19	121	18	1,381	7,672	900	9,971	366	764								
Atmospheric deposits	Leaves		ng/g	2,988	5,648	648	2,340	483	112	469	69	373	76	214	31	191	29	2,217	12,219	1,423	15,888	612	648								
Atmospheric deposits	Leaves		ng/g	2,539	4,765	570	2,144	423	100	410	55	331	64	173	25	180	26	1,829	10,540	1,239	13,633	560	825								
TDSD1[a]			µg/g	45.2	89.4	10.3	38.4	7.13	1.22	6.05	0.84	4.22	0.80	2.16	0.31	1.92	0.28	20.7	192	16	229	18.5	NM								
TDSD2[a]			µg/g	37.7	76.7	9.2	34.2	6.96	1.15	5.97	0.85	4.66	0.88	2.34	0.33	2.07	0.31	19.0	166	17	202	17.2	NM								
TDSD3[a]			µg/g	34.0	64.1	8.5	31.1	6.17	1.02	5.00	0.72	4.13	0.80	2.18	0.32	1.99	0.29	17.0	145	15	177	13.0	NM								
UCC			µg/g	*31.00*	*63.00*	*7.10*	*27.00*	*4.70*	*1.00*	*4.00*	*0.70*	*3.90*	*0.83*	*2.30*	*0.30*	*1.96*	*0.31*	*21.00*	134	14	169	*10.50*	*2.70*					1.00	1.00	1.00	1.00
	Herbs		µmol/kg	1.15	1.28	0.21	0.78	0.18	0.03	0.26	0.04	0.12	0.03	0.06	0.01	0.04	0.00	1.01				0.16	0.01	0.9	BDL		19,871				
	Leaves	av.	µmol/kg	6.30	2.71	0.84	2.83	0.48	0.13	0.44	0.05	0.22	0.04	0.08	0.01	0.06	0.01	2.20				0.22	0.01	1.0	BDL		22,484				
		±σ		1.79	0.87	0.40	1.33	0.19	0.06	0.18	0.02	0.07	0.02	0.04	0.01	0.03	0.01	0.77				0.14	0.01				12,342				
		kg/ha/yr																													
	Herbs	1,601	mmol/km²/yr	184	205	33	124	29	5	41	6	19	5	9	1	7	0	161	580	89	830	26	2	145	BDL	mol/km²/yr	3,180				
	±σ	±88		10	11	2	7	2	0	2	0	1	0	1	0	0	0	9	32	5	46	1	0	8			176				
	Leaves	3,415	mmol/km²/yr	2,150	926	286	966	165	46	151	18	75	14	28	3	20	5	751	4,539	312	5,601	75	4	343	BDL	mol/km²/yr	7,678				
	±σ	±816		514	221	68	231	39	11	36	4	18	3	7	1	5	1	179	1,085	75	1,338	18	1	82			1,835				
	Total	5,016	mmol/km²/yr	2,334	1,131	319	1,090	194	51	192	23	94	19	38	4	26	5	912	5,119	401	6,431	101	6	488	BDL	mol/km²/yr	10,858				
	±σ	±904		524	233	70	238	41	11	38	5	19	4	7	1	5	1	188	1,117	79	1,384	19	1	90			2,010				
	% herbs			8	18	10	11	15	9	21	24	21	28	25	29	25	5	18	11.3	22.2	12.9	26	32	30			29				

[a]The HFSE analyses of the Thar atmospheric dust (TDSD) are from Ferrat et al. (2011). The estimate of the litter-associated elemental fluxes are calculated with the average and standard deviation of the litter dry masses of herbs and leaves (years 2009 and 2010) given in Table 3 from Riotte et al. (2014a).

AGU Geochemistry, Geophysics, Geosystems

10.1002/2017GC007158

Table 3

Average Concentrations of REY-Th-U, Sums and UCC-Normalized Ratios [LREE/HREE, Ce/Ce, Eu/Eu, $(La/Sm)_N$, and $(Gd/Yb)_N$] for the Wet Atmospheric and Throughfall Deposits (WAD and TFD), Overland Flow Water (OFW), Soil Pore Water, i.e., Seepages, (SPW), Groundwater From BH1, BH5, and BH6 (GDW1–2-3) and Stream Water at Outlet (OSW)

Sample	Abbr.	Stat.	*n*	*T* (°C)	pH	Conductivity (µS/cm)	Alkalinity (µmol/L)	DOC (mg/L)	La (µg/L)	Ce (µg/L)	Pr (µg/L)	Nd (µg/L)	Sm (µg/L)	Eu (µg/L)	Gd (µg/L)	Tb (µg/L)	Dy (µg/L)	Ho (µg/L)	Er (µg/L)	Tm (µg/L)	Yb (µg/L)	Lu (µg/L)	Y (µg/L)	Th (µg/L)	U (µg/L)	LREE	HREE	REE (µg/L)	%LREE (%)	LREE/ $HREE_N$	Ce/ Ce	Eu/ Eu	La/ Sm_N	Gd/ Yb_N
Wet atmospheric deposits	WAD	Average	34	NM	6.38	22.4	NM	1.0	0.010	0.024	0.003	0.012	0.003	0.002	0.004	0.001	0.002	0.001	0.002	0.001	0.001	0.001	0.009	0.005	0.001	0.054	0.013	0.067	80	0.43	1.03	2.86	0.53	1.26
		Min			5.87	5.5		0.5	BDL	0.002	BDL	BDL	BDL	BDL	BDL	BDL	BDL	BDL	BDL	BDL	BDL	BDL	0.002	BDL	BDL	BDL	BDL	BDL						
		Max			6.71	57.0		2.7	0.139	0.281	0.037	0.144	0.023	0.007	0.026	0.003	0.015	0.003	0.009	0.001	0.007	0.001	0.021	0.018	0.005	0.630	0.066	0.696	90	1.02	0.92	1.14	0.90	1.78
		±σ			*0.28*	*11.1*		*0.5*	*0.023*	*0.049*	*0.006*	*0.023*	*0.004*	*0.002*	*0.005*	*0.001*	*0.003*	*0.001*	*0.002*	*0.000*	*0.001*	*0.000*	*0.006*	*0.005*	*0.001*			*0.115*						
Troughfall deposits	TFD	Average	14	NM	7.00	83.5	705	34.3	0.056	0.097	0.015	0.061	0.015	0.006	0.012	0.002	0.011	0.003	0.007	0.005	0.005	0.003	0.060	0.008	0.004	0.249	0.049	0.298	84	0.55	0.80	1.94	0.55	1.17
		Min				27.0	154	10.0	0.006	0.023	BDL	0.014	0.003	BDL	BDL	BDL	0.002	BDL	BDL	BDL	BDL	BDL	0.015	0.002	BDL	BDL	BDL	BDL						
		Max				140.0	1,591	134.9	0.199	0.331	0.054	0.232	0.059	0.019	0.060	0.011	0.049	0.012	0.032	0.007	0.024	0.008	0.210	0.031	0.013	0.894	0.204	1.098	81	0.47	0.75	1.38	0.51	1.25
		±σ				*79.9*	*590*	*37.3*	*0.057*	*0.092*	*0.015*	*0.061*	*0.016*	*0.006*	*0.016*	*0.004*	*0.012*	*0.004*	*0.009*	*0.004*	*0.007*	*0.003*	*0.055*	*0.008*	*0.003*			*0.290*						
Overland flow water	OFW	Average	18	NM	6.79	56.5	346	7.8	0.534	0.655	0.127	0.572	0.116	0.025	0.115		0.094	0.017	0.054	0.006	0.048	0.006	NM	0.016	0.016	2.029	0.340	2.369	86	0.64	0.59	0.94	0.70	1.18
		Min			5.94	31.0	158	4.3	0.202	0.197	0.043	0.204	0.039	0.009	0.038		0.031	0.006	0.020	0.000	0.015	0.001		0.002	0.005	0.694	0.112	0.806	86	0.66	0.50	0.95	0.78	1.21
		Max			7.71	121.0	761	12.9	1.031	1.384	0.256	1.178	0.243	0.054	0.250		0.201	0.038	0.116	0.016	0.110	0.015		0.030	0.040	4.147	0.746	4.893	85	0.59	0.63	0.95	0.64	1.12
		±σ			*0.48*	*21.2*	*145*	*2.5*	*0.242*	*0.324*	*0.059*	*0.269*	*0.056*	*0.013*	*0.057*		*0.047*	*0.009*	*0.026*	*0.004*	*0.024*	*0.004*		*0.009*	*0.008*			*1.119*						
Soil pore_water 1	SPW1	Average	4	NM	NM	247.0	NM	NM	0.113	0.098	0.031	0.144	0.034	0.007	0.029		0.022	0.004	0.015	0.001	0.014	0.002	NM	0.019	0.048	0.427	0.087	0.514	83	0.53	0.39	0.96	0.51	1.02
Soil pore_water 2	SPW2	Average	4		7.31	152.5	837	NM	0.388	0.312	0.097	0.430	0.090	0.022	0.083		0.069	0.013	0.038	0.004	0.034	0.005	NM	0.006	0.027	1.339	0.246	1.585	84	0.58	0.38	1.12	0.65	1.18
Soil pore_water 3	SPW3	Average	7		7.32	87.9	619	5.7	0.333	0.500	0.091	0.417	0.080	0.018	0.080		0.066	0.012	0.041	0.004	0.041	0.005	NM	0.019	0.016	1.440	0.249	1.689	85	0.62	0.68	0.95	0.63	0.95
		Average	15		7.31	140.5	728	5.7	0.289	0.343	0.076	0.348	0.071	0.016	0.067		0.055	0.010	0.033	0.004	0.032	0.004		0.015	0.032	1.143	0.205	1.348	85	0.60	0.54	1.01	0.62	1.03
		Min			6.71	59.3	242	2.4	0.061	0.068	0.016	0.081	0.017	0.003	0.014		0.011		0.007		0.005			0.003	0.012	0.246	0.038	0.283	87	0.70	0.51	0.83	0.53	1.35
		Max			7.84	327.0	1,260	9.7	0.996	1.728	0.287	1.299	0.245	0.058	0.245		0.201	0.042	0.126	0.017	0.133	0.021		0.040	0.067	4.614	0.785	5.398	85	0.63	0.89	1.14	0.76	1.20
		±σ			*0.29*	*76.3*	313	*2.4*	*0.239*	*0.413*	*0.067*	*0.301*	*0.057*	*0.014*	*0.057*		*0.047*	*0.010*	*0.029*	*0.004*	*0.030*	*0.005*		*0.011*	*0.021*			*1.249*			*0.23*	*0.15*	*0.08*	*0.13*
Valley																																		
Groundwater (BH1)	GDW1	Average	8	25.0	7.05	229.3	1,658	2.0	0.035	0.050	0.007	0.032	0.004	0.003	0.007		0.005	0.001	0.005	0.001	0.005	0.001	0.057	BDL	0.928	0.133	0.025	0.158	84	0.56	0.74	2.50	1.37	0.74
Ridgetop																																		
Groundwater (BH5)	GDW2	Average	9	24.9	7.66	667.9	5,614	BDL	0.011	0.016	0.002	0.012	0.003	0.005	0.005		0.006	0.002	0.007	0.000	0.007		0.132	BDL	0.441	0.049	0.027	0.076	65	0.20	0.73	5.27	0.49	0.34
Groundwater (BH6)	GDW3	Average	10	25.0	7.67	899.8	6,716	BDL	0.013	0.017	0.003	0.014	0.003	0.002	0.005		0.007	0.002	0.009	0.001	0.014	0.003	0.116	BDL	1.384	0.051	0.041	0.093	56	0.13	0.72	4.17	1.59	0.15
		Average	19	25.0	7.66	789.9	6,194		0.012	0.016	0.003	0.013	0.003	0.003	0.005		0.007	0.002	0.008	0.001	0.010	0.002	0.123	BDL	0.937	0.050	0.035	0.085	59	0.15	0.75	5.50	1.16	0.22
		Min		24.2	6.92	622.0	4,392		0.003	0.004	0.001	0.003	0.000	0.000	0.001		0.001	0.001	0.002	0.000	0.004	0.001	0.051		0.308	0.012	0.010	0.022	54	0.13	0.31	0.70	0.11	0.06
		Max		26.4	8.60	981.0	10,545		0.042	0.045	0.008	0.036	0.006	0.008	0.012		0.019	0.006	0.021	0.002	0.034	0.008	0.303		2.166	0.145	0.102	0.247	59	0.15	1.28	25.52	9.68	0.39
		±σ		*0.9*	*0.46*	*127.2*	*1,475*		*0.009*	*0.011*	*0.002*	*0.008*	*0.002*	*0.002*	*0.003*		*0.004*	*0.001*	*0.005*	*0.000*	*0.007*	*0.002*	*0.060*		*0.560*			*0.047*			*0.27*	*7.11*	*2.11*	*0.11*
Stream water (Mule Hole)	OSW	Average	130	25.4	6.97	74.2	555	8.0	0.391	0.592	0.098	0.423	0.089	0.022	0.079	0.011	0.071	0.014	0.044	0.006	0.040	0.006	0.401	0.035	0.018	1.615	0.272	1.887	86	0.63	0.71	1.12	0.66	0.97
		Min	23.3	5.95	34.0	161	3.2	0.065	0.017	0.016	0.093	0.024	0.006	0.021	0.003	0.018	0.003	0.012		0.011		0.131	0.007	0.003	0.221	0.068	0.289	76	0.35	0.09	0.78	0.42	0.43
		Max	27.9	8.00	191.0	3,432	17.3	1.220	1.836	0.310	1.329	0.283	0.060	0.264	0.032	0.223	0.042	0.129	0.017	0.113	0.016	1.102	0.107	0.055	5.038	0.836	5.874	86	0.64	1.00	1.63	1.11	1.17
		±σ	*1.1*	*0.40*	*28.1*	*323*	*2.3*	*0.196*	*0.350*	*0.050*	*0.212*	*0.044*	*0.011*	*0.040*	*0.006*	*0.035*	*0.007*	*0.021*	*0.003*	*0.019*	*0.003*	*0.211*	*0.015*	*0.009*			*0.997*			*0.16*	*0.15*	*0.08*	*0.10*

The solute chemistry of throughfall deposits reflects the effects of canopy-dependent processes as they represent the portion of the bulk rainfall that drips from the forest canopies (Bhat et al., 2011). Tree canopy acts as a source or sink for rain solutes, i.e., leached from the foliage or absorbed by leaves (Potter et al., 1991).

The overland flow water samples ($n = 20$) were collected from 2009 to 2011 over the ferralsol cover and over the vertisol-ferralsol transition cover (for more details see Riotte et al., 2014a) using a PVC pipe on the ground and a buried container. Each sample integrates 2–3 weeks of punctual overland flow. In 2004, a swamp water sample was also collected above the vertisol cover. The soil pore waters ($n = 11$) were collected along the Mule Hole stream bank close to the watershed's reference soil catena (Barbiéro et al., 2007). The soil pore water from the vertisol was collected in 2004 while those of the ferralsol-vertisol transition were collected in 2009 and 2010.

The groundwater samples were collected in the piezometer network. Two kinds of groundwater were analyzed. (i) From the ridge top boreholes BH5 and BH6 (GDW2, GDW3) which were only fed by the direct recharge and (ii) from the borehole BH1 (GDW1) located at the watershed outlet which was partially fed by indirect recharge from the stream (Maréchal et al., 2009, 2011). The ridge top groundwater floods the deeper layers of the regolith (fractured bedrock). The groundwater slowly discharges out of the watershed as underflow without contributing to the stream flow (Riotte et al., 2014b).

The water samples for trace element studies were collected in 1 N HCl cleaned polypropylene bottles and acidified with double-distilled HNO_3. The REY-Th-U concentrations were measured by ICP-MS Elan 6000 at Geosciences Environnement Toulouse (GET, France) in the same conditions as described for plant samples, i.e., using In and Re as internal standards and EPONDU-4 and SLRS-4 or SLRS-5 as external ones. The precision of ICPMS data are about 10%. Dissolved organic carbon was determined with a TOC analyzer Shimadzu (TOC 5000).

3.3. Data Handling: Modeling of Hydrological Fluxes

The lumped hydrological model developed for the Mule Hole watershed (Violette et al., 2010a) has been modified to consider canopy interception and the long-term average rainfall (Riotte et al., 2014a). Both hydrological budget and field observations at the Mule Hole CZO indicate that apart from the vicinity of the stream where some overland flows occur, the whole flux passing through the canopy infiltrates without significant evaporation. Then, on the hill slopes, the water balance can reasonably be computed on 1-D vertical profile. The model is a reservoir model designed to simulate on an hourly basis combining the water storage on canopy leaves, in soil, in saprolite and the exchange flows between these reservoirs. The forcing parameters such as rainfall (P) and potential evapotranspiration (PET) are measured by the micrometeorological station. The total actual evapotranspiration (AET) is computed from the canopy interception (Inter), the soils (Ep), and saprolite (Ea) according to available water with the following equation:

$$\mathrm{AET} = \mathrm{Inter} + \mathrm{Ea} + \mathrm{Ep} \leq \mathrm{PET} \tag{1}$$

This provides a way to consider deep root water uptake by the forest. This triple-box model was replicated for ferralsol and vertisol profiles. At the scale of the watershed, the water balance can be described as

$$\mathrm{P} = \mathrm{AET} + \mathrm{Q_{stream}} + \mathrm{R} + \Delta\mathrm{S} \tag{2}$$

where $\mathrm{Q_{stream}}$ = stream flow, R = groundwater recharge, and ΔS = change in soil water stock. The total flows are weighted according to the respective surface areas of ferralsol and vertisol. The simulated runoff at the outlet, calculated as

$$\mathrm{Q_{stream}} = \mathrm{Q_{OF}} + \mathrm{Q_{seepage}} \tag{3}$$

has been used for the model calibration, with $\mathrm{Q_{OF}}$ the flux from the overland flow and $\mathrm{Q_{seepage}}$ the flux from the soil layer (inter flow). The flow to the aquifer is constrained to match with yearly estimates of the total recharge that is obtained from the chloride mass balance method for the period of 2004–2006 (Maréchal et al., 2009). The water budget at the scale of 1-D soil-plant profile can be described as

$$\mathrm{P} = \mathrm{Inter} + \mathrm{Q_{ground}} \tag{4}$$

where $\mathrm{Q_{ground}} = \mathrm{Q_{OF}} + \mathrm{Q_{soil\ input}}$ and $\mathrm{Q_{soil\ input}}$ is the water flux infiltrating into the soil layer. Within the soil,

part of this flux can be evaporated (Ep), the other ($Q_{soil\ output}$) leaves the soil either toward the stream ($Q_{seepage}$) or toward the saprolite ($Q_{saprolite}$):

$$Q_{soil\_input} = Q_{soil\_output} + Ep = Q_{seepage} + Q_{saprolite} + Ep \quad (5)$$

The equations used to calculate the fluxes of an element j (F_j) with the concentration of j and the output of the hydrological model for each ecosystem compartment are summarized in Table 1, i.e., for above ground ($F_{j,atmospheric\_input}$, $F_{j,throughfall}$, $F_{j,ground}$, $F_{j,canopy\_interaction}$, and $F_{j,vegetation\_cycling}$), for soil ($F_{j,soil\_input}$, $F_{j,soil\_output}$), for groundwater ($F_{j,groundwater}$) and for stream ($F_{j,discharge}$). The equations are developed in Riotte et al. (2014a).

4. Results

4.1. Vegetation: Dry Litter Composition and Budget (Leaves and Herbs) and Associated Dry Atmospheric Deposits

Table 2 reports the REY-Th-U, Ti, Zr, and P content in the litter (leaves and herbs) from the ATT facies and in the atmospheric deposits composed of geogenic particles and plant debris. The estimate of raw litter-associated fluxes of elements are calculated with the average and standard deviation of the litter dry masses of herbs and leaves (years 2009 and 2010) given in Table 3 from Riotte et al. (2014a). The tree leaves are richer in REY than grass containing 2,200 and 690 ng/g, respectively. The UCC-normalized patterns (Figure 2) indicate a moderate enrichment of the lighter REE ($La/Sm_N = 1.8 \pm 0.2$), and a strong HREE depletion ($Gd/Yb_N = 3.0 \pm 1.1$), significant negative Ce-anomalies that are more pronounced for tree leaves ($Ce/Ce^* = 0.3 \pm 0.1$) than for grass ($Ce/Ce^* = 0.6$), and significant Y enrichment. The Eu-anomaly is slightly positive for tree leaves with Eu/Eu* ranging from 1.0 to 1.3 while, it is negative for grass ($Eu/Eu^* = 0.6$). The estimates of the whole elemental fluxes (in $mmol/km^2/yr$) are of 5,120 ± 1,120 for LREE (11% for grass), 400 ± 80 for HREE (22% for grass), and 910 ± 190 for Y (18% for grass). The tree leaves and grass are richer in Th (range 25–98 ng/g) than U (range 1.6–6.3 ng/g) with whole fluxes (in $mmol/km^2/yr$) of 100 ± 20 (26% for grass) and 6 ± 1 (32% for grass) for Th and U,

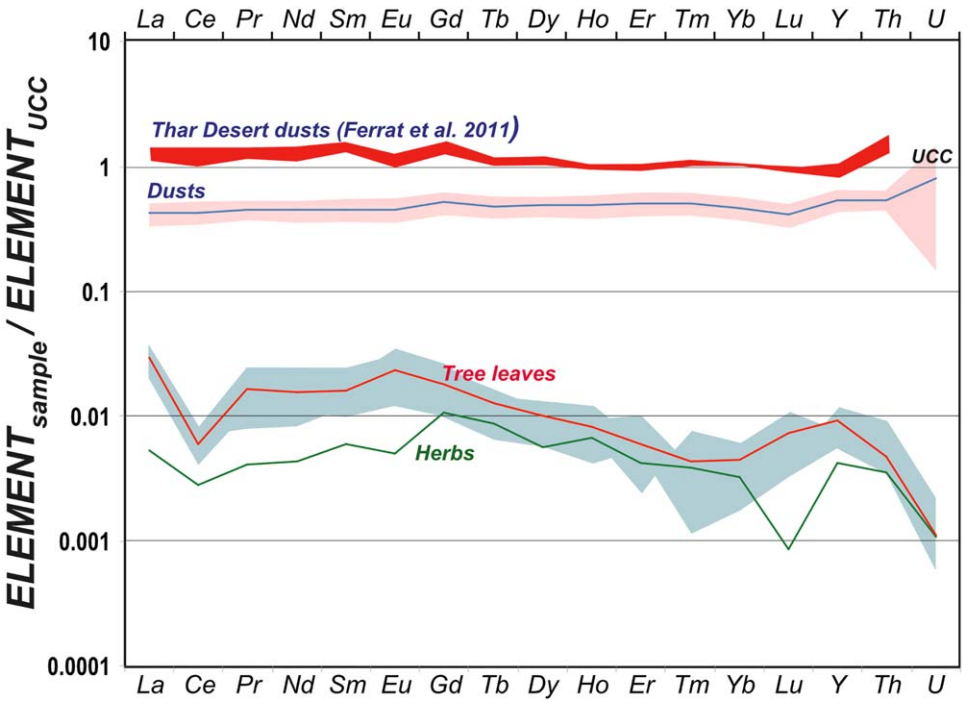

Figure 2. UCC-normalized REY-Th-U patterns of leaves and herbs from litter and associated atmospheric dusts. The geogenic REY-Th-U signature of the particles is estimate with a linear regression model assuming that (i) 100% of Al of the blend is of geogenic origin and (ii) the end-member composition of the dust aerosols ("pure" dust component) is similar to the Thar Desert dust composition (Al = 6.4 ± 1.2%; Yadav & Rajamani, 2004). The shadow regions represent the variability.

respectively. The P content is highly variable from one species to another, ranging from 0.4 to 1.1 mg/g in *T. grandis* and *T. crenulata* leaves, respectively, and 0.6 mg/g in *T. triandra* grass. The whole P flux is 10,860 ± 2,010 mol/km^2/yr (29% from grass). The Ti content is below the detection limit while the Zr content is significant, ranging from 70 to 130 ng/g with a whole flux of 500 ± 90 mmol/km^2/yr (30% from grass).

The property-property graphs (Figure 3) display a strong positive correlation for La (LREE), Y (HREE), and Th but a weak correlation for U with respect to Al. The relationships between elements versus Al allow us to estimate the REY and Th contents of the geogenic dust at Mule Hole and conversely the dust-free composition of vegetation. This estimation is not possible for U due to the absence of correlation with Al. Both the UCC-normalized Mule Hole and Thar Desert dusts (Figure 2) display flat patterns, but REE concentrations of Mule Hole dusts are slightly lower than those of the Thar Desert.

4.2. Hydrological Balance, Solute Water Chemistry, and Contemporary Fluxes

Table 3 reports the standard statistics for the REY-Th-U concentrations, pH, alkalinity, conductivity, dissolved organic carbon (DOC), and the specific ratios in (i) the wet atmospheric and throughfall deposits, (ii) the overland flow and soil pore waters, and (iii) groundwater. The Upper Continental Crust composition is used for the normalization of the different solutes (Figure 4). Table 4 summarizes the solute flux estimates for LREE, HREE, U, Th, and DOC for (i) the soil-plant profile (ferralsol), (ii) the ridge top groundwater, and (iii) the Mule Hole stream. The hydrological model-based approach presented in Riotte et al. (2014a) is used to estimate the solute fluxes of LREE, HREE, Y, U, and Th coming from (i) the atmospheric inputs, (ii) the interactions with canopy and forest floor, and (iii) the mineral chemical weathering. For the present paper, the calculation of solute groundwater fluxes was based on the lowest groundwater discharge estimate of 45 mm/yr (Marechal et al., 2009).

4.3. Wet Atmospheric and Throughfall Deposits

The wet atmospheric deposit chemistry is characterized by slightly acidic pH (6.4 ± 0.3), very low conductivity (22 ± 11 μS/cm), and low DOC concentration (1.0 ± 0.5 mg/L) while throughfall deposit chemistry exhibits neutral pH, moderate conductivity (83 ± 80 μS/cm), and high and variable DOC concentration (34 ± 37 mg/L). The REY-Th-U concentrations are extremely variable and often below detection limit in both wet atmospheric and throughfall deposits. The UCC-normalized patterns do not show significant

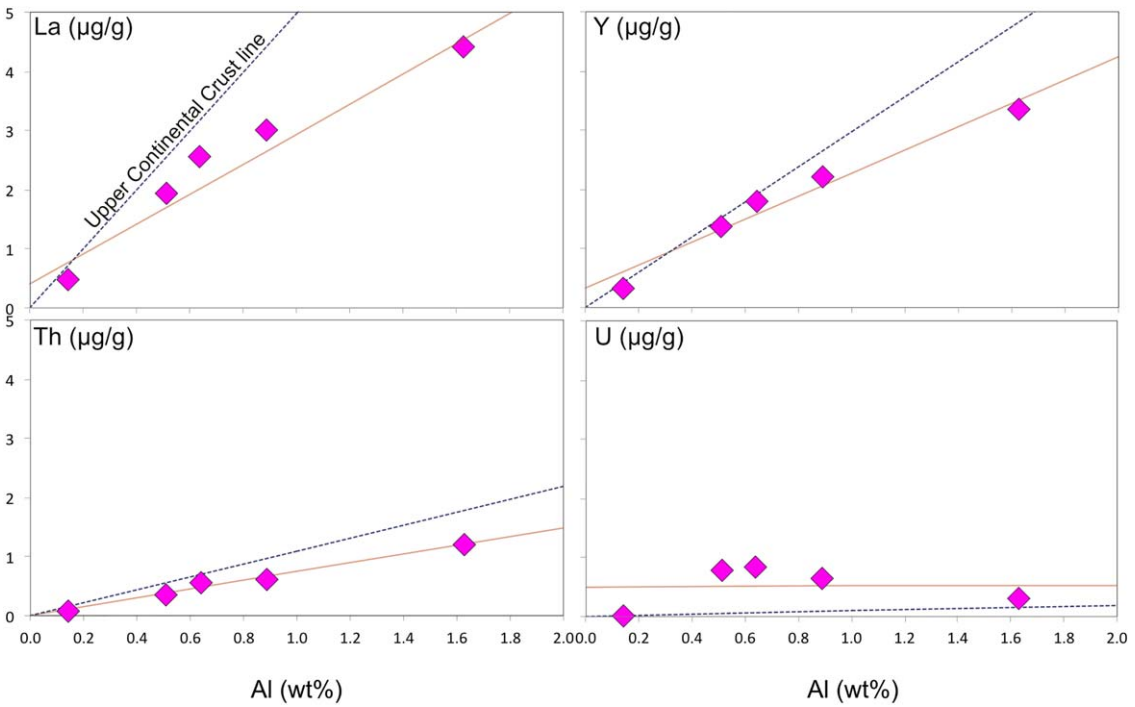

Figure 3. Property-property graphs represent Al content versus La, Y, Th, and U content in the dry atmospheric deposits collected by washing leaves and herbs from litter. The Upper Continental Crust line is reported.

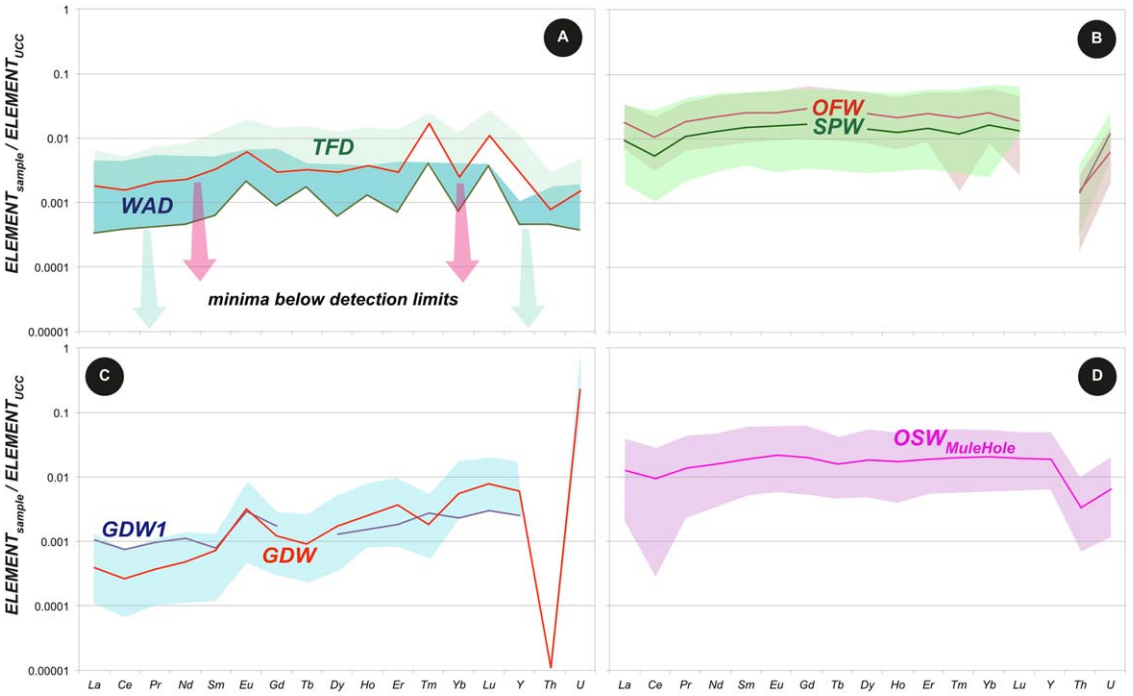

Figure 4. UCC-normalized REY-Th-U patterns for (a) wet atmospheric and throughfall deposits, (b) soil inputs (overland flow water) and soil outputs (soil pore waters), (c) stream water, and (d) groundwater. The shadow regions represent the variability.

fractionations or anomalies (Figure 5a). Wet atmospheric deposit fluxes are extremely low while the effects of canopy-dependent processes significantly increase the throughfall deposit fluxes of LREE, HREE, U, and Th (Table 4). The canopy interaction (in %), which includes dust leaching, is calculated as the average fluxes of throughfall deposits minus wet atmospheric deposits. It shows an enrichment of about 76% for LREE, 70% HREE, 73% for U, and only 35% for Th (Table 4).

Table 4
Solute Mass Balance at the 1-D Soil-Plant Profile Scale (Ferralsol) for LREE, HREE, Th, and U

		Water budget (mm/yr)	±σ	LREE (mmol/km²/yr)	±σ	HREE (mmol/km²/yr)	±σ	Th (mmol/km²/yr)	±σ	U (mmol/km²/yr)	±σ	DOC (kg/km²/yr)	±σ
Above ground	*Fj_wet atm. inputs*	*1,100*	250	415	21	8.9	0.4	22	1	4.5	0.2	1,150	57
	Fj_throughfall	*994*	102	1,749	179	29.4	3.0	34	4	17	2	34,098	3,499
	Fj_ground	*994*	102	14,236	1,461	206.9	21.2	69	7	67	7	7,724	793
	Fj_canopy interaction			**1,333**	0	**204**	0.0	**12**		**12**		**32,949**	
	Canopy interactions (%)			*76*		*70*		*35*		*73*		*97*	
	Fj_forest floor interactions			**13,820**	0	**1,980**	0.0	**46**		**63**		**6,574**	
	Forest floor interactions (%)			*97*		*96*		*67*		*93*		*85*	
	Fj_litter decay			5,120	1,120	400	80	101.0	19.0	6.0	4.0		
	Fj_atmospheric dusts			9,116	1,841	1,669	227	−32.3	20.3	61.3	8.0		
	% brought by dust			*64*		*81*		*−47*		*91*			
Soil	*Fj_soil input*	*925*	*213*	13,247	3,050	1,926	443	64.0	14.7	63	14	7,188	1,655
	Fj_soil_output	*187*	*37*	1,507	298	235	46	12.3	2.4	25	5	1,068	211
	ΔFj_soil	*−738*		**−11,741**	**3,065**	**−1,691**	**446**	**−52**	**15**	**−38**	**15**	**−6,120**	**1,669**
	Soil cycling (%)	*−80*		*−89*		*−88*		*−81*		*−60*		*−85*	
Stream	*Fj_stream_output*	*94*	*19*	1,072	217	157	32	14	3	7.0	1.4	7,529	1,522
Groundwater	*Fj_grdw_output*	*45*	*9*	16	3	9	2	BDL		177	35	BDL	

Note. The export fluxes are indicated for the Mule Hole groundwater and stream. The estimated fluxes are calculated with the average water concentrations (Table 3) and the results of the water budget for the ferralsol profile (Riotte et al., 2014a, 2014b) and for the groundwater (Maréchal et al., 2009). The errors are calculated with the standard deviation of the water fluxes.

4.4. Overland Flow Waters and Soil Pore Water

The features of the overland flow chemistry have circumneutral pH (6.8 ± 0.5), low conductivity (56 ± 21 μS/cm), low alkalinity (350 ± 145 μmol/L), and moderate DOC concentrations (7.8 ± 2.5 mg/L). The REE concentration in overland flow is ranging from 810 to 4,890 ng/L (average 2,370 ng/L; 86% LREE). Deduced soil input fluxes of LREE and HREE are 13,250 and 1,930 mmol/km^2/yr, respectively. Average U and Th concentration is 16 ng/L, leading to soil input fluxes of 60 mmol/km^2/yr. The average UCC-normalized REY-Th-U pattern is nearly flat with a significant negative Ce-anomaly (Ce/Ce* = 0.60) and Th depletion.

The characteristics of the soil pore water chemistry have circumneutral pH (7.3 ± 0.3), moderate conductivity (140 ± 80 μS/cm), alkalinity (730 ± 310 μmol/L), and moderate DOC concentration (5.7 ± 2.4 mg/L). The REE concentrations are high and vary widely between 290 and 5,400 ng/L (average 1,350 ng/L; 85% LREE) leading to soil output fluxes of LREE and HREE of 1,507 and 235 mmol/km^2/yr, respectively. Average U and Th concentrations in soil pore water are 32 ± 21 and 15 ± 11 ng/L, respectively, and corresponding soil output fluxes are 25 and 12 mmol/km^2/yr, respectively. The average UCC-normalized REY-Th-U pattern shows slight HREE enrichment with a significant negative Ce-anomaly (Ce/Ce* = 0.53) and Th depletion similar to the overland flow water (Figure 5b). The comparison between the soil output and input fluxes indicates that 90% of REE, 81% of Th, and only 60% of U are removed from pore water in the soil layers (Table 4).

4.5. Stream Water

Circumneutral pH (7.0 ± 0.4), low conductivity (74 ± 28 μS/cm), moderate alkalinity (550 ± 320 μmol/L), and significant DOC concentration (8.0 ± 2.3 mg/L) characterize the Mule Hole stream chemistry. The UCC-normalized REY-Th-U patterns show a significant negative Ce-anomaly (Ce/Ce* = 0.72) and a slight Th depletion (Figure 5d). The sum of the REE concentrations of the stream (av. 1,900 ng/L, 86% LREE) is in the same range compared to those of overland flow and soil pore waters. The U concentration (av. 18 ng/L) and

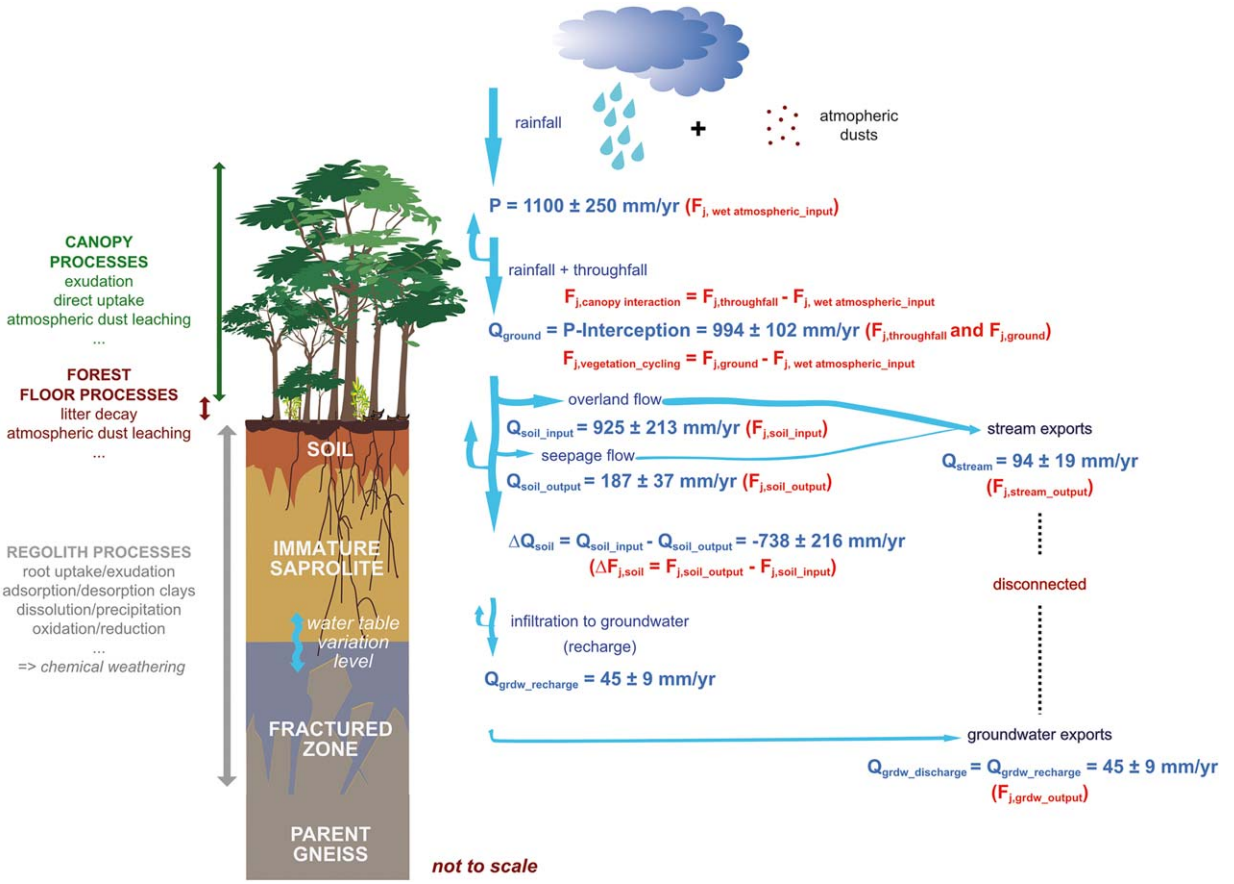

Figure 5. Conceptual model, water balance, and elemental flux equations at the soil profile scale (ferralsol) indicating (i) solute sources, (ii) processes for regolith (soil and saprolite), canopy, and forest floor.

the Th concentration are significant (av. 35 ng/L) with respect to those of groundwater. The LREE, HREE, U, and Th stream fluxes are 1,070, 160, 7, and 14 mmol/km^2/yr, respectively (Table 4).

4.6. Groundwater

The principal characteristics of the ridge top groundwater are circumneutral pH (7.7 $\pm$ 0.5), high conductivity (790 $\pm$ 130 μS/cm), elevated alkalinity (6,190 $\pm$ 1,470 μmol/L), and DOC concentration always close or below the detection limit (0.2 mg/L). The concentrations are very low for REE (90 ng/L; 59% LREE), significant for Y (120 ng/L), the highest at the watershed scale for U (940 ng/L), and below detection limit for Th ($<$1 ng/L). The UCC-normalized patterns (Figure 5c) show a pronounced HREE enrichment, a huge positive Eu-anomaly (Eu/Eu* = 5.6), a slight negative Ce-anomaly (Ce/Ce* = 0.75), a strong Th depletion, and a huge U enrichment. In comparison, the groundwater partially fed by the brook (GDW1) has lower conductivity (229 $\pm$ 30 μS/cm), lower alkalinity (1,660 $\pm$ 400 μmol/L), and higher DOC (2.0 $\pm$ 0.4 mg/L). The concentrations are higher for REE (158 ng/L; 84% LREE), lower for Y (67 ng/L), of the same magnitude for U (930 ng/L) and always below detection limit for Th ($<$1 ng/L). The LREE and HREE fluxes exported through the groundwater are very low (16 and 9 mmol/km^2/yr, respectively; 50 and 20 times less than those of stream water) but high for U (180 mmol/km^2/yr; 25 times higher than that of the stream; Table 4). Th is not mobilized by groundwater.

5. Discussion

5.1. Contemporary Solute Mass Balance at the Scale of the Ferralsol Profile

Figure 5 displays the conceptual model, water balance, and elemental flux equations at the soil profile scale (ferralsol). The HFSE solute sources and processes for regolith (soil and saprolite), canopy, and forest floor are also indicated.

5.1.1. Above the Ground

At Mule Hole, both canopy and forest floor processes have a significant effect on the enrichment of REY-Th-U and dissolved organic matter in the above-ground solutions, leading to a higher potential to mobilize HFSE by chelation. In throughfall deposits and overland flow water, the average DOC fluxes are 34,100 and 7,720 kg/km^2/yr, respectively. The average REY-Th-U fluxes increase from (i) wet atmospheric deposits to throughfall deposits due to the addition of solutes resulting from canopy interactions and (ii) from throughfall deposits to overland flow due to the addition of solutes coming from litter decay. Nevertheless, the average fluxes of LREE, HREE and U (in mmol/km^2/yr) to the ground calculated with the overland flow water composition (14,240 for LREE, 210 for HREE, and 67 for U, Table 4) are quite higher than the maximum fluxes expected from the complete litter decay during the water year (5,120 for LREE, 400 for HREE, and 6 for U, Table 2). The dust leaching contributing to the above-ground solution is at least 60% for LREE and 80% for HREE (Table 4). This contribution is less obvious for Th with quite similar fluxes from forest floor processes and litter decay (70 against 100 mmol/km^2/yr) due to its comparatively immobile nature.

5.1.2. Origin of the Solutes in the Soil Output Flux

Substantial amount of soluble REE-Th-U is brought to the soil layers by both canopy and forest floor processes ($F_{j\_soil\ input}$ of 13,250 mmol/km^2/yr of LREE, 1,930 mmol/km^2/yr of HREE, 60 mmol/km^2/yr of U and Th, Table 4). The elements are mostly chelated by organic ligand produced by the litter decay. In the ferralsol layers, the elemental recycling reaches about 90% for REE whereas it is lower for Th (80%) and for U (60%). In case of Ca, Mg, Si, and K, root uptake is likely responsible for the remobilization of the elements toward the vegetation cycle. Root uptake controls the transfer of soluble REE-Th-U from the soil toward the deeper groundwater reservoir at least by default through the water balance (Ruiz et al., 2010), but likely also transfers the soluble elements through mineral dissolution and uptake in proportions that are impossible to assess from an input-output mass balance. Sorption of U(VI) on Fe-oxide minerals (such as hematite [αFe2O3] and goethite [αFeOOH]) and occlusion of U(VI) by Fe-oxide coatings are also processes that can retard U transport in environments and limit its biological availability (Duff et al., 2002).

5.2. Export by the Groundwater

The groundwater chemistry is related to both recharge water chemistry and water-rock interactions. Present-day groundwater solute exports are noteworthy for U (25 times more than the stream export) and very low for LREE and HREE (50 and 20 times less than the stream export, respectively) and nil for Th (Table 4). Accordingly, Th is inert in the saprolite where it is likely immobilized within iron oxides and oxyhydroxides or precipitated as thorianite (ThO_2; Braun et al., 1993; Langmuir & Herman, 1980). The REY-U stock

released from the breakdown of reactive accessory minerals is then likely incorporated into authigenic minerals such as phosphates, carbonates and oxides, or adsorbed/occluded on/in clays and clay minerals (Braun et al., 1998; Laveuf et al., 2008; Duff et al., 2002; Laveuf & Cornu, 2009). Owing to DOC-free groundwater preventing the significant formation of organic chelates, the geochemical processes, potentially catalyzed by bacterial activity (Takahashi et al., 2005; Taunton et al., 2000) govern the water/rock/saprolite interactions. In an environment with circumneutral pH and mostly oxidizing conditions, the expected precipitated REY-U phases would be phosphates such as rhabdophane and florencite. Addition of REY-U by percolating fluids can also lead to the formation of these authigenic minerals following the model proposed in (Braun et al., 1998). The large but highly variable positive Eu-anomaly (Eu/Eu* = 5.5) of groundwater can be attributed to the effective dissolution of plagioclase at the weathering front. In oxidizing environments, U is mostly soluble and mobile in the hexavalent oxidation state. The regolith profile developed over the Coles Hill uranium deposit (Virginia, USA; Jerden et al., 2003) showed that U transport may be inhibited or naturally attenuated by the precipitation of U(VI) phosphate minerals in oxidizing and saturated soil environments. These phosphates are however unstable and their dissolution leads to the U leaching.

Overall, the groundwater leaching from the Mule Hole saprolite is weak for both LREE and HREY and nil for Th. The only element to be significantly mobilized and leached is U, mostly due to the primary U-bearing mineral breakdown. Contrary to the soil layers, the alkalinity of groundwater is high. The low amount of iron-related secondary minerals prone to U-adsorption in both saprock and saprolite and the extremely low vegetation uptake in deep regolith zone are in favor of the preferential leaching of U at Mule Hole. However, the precipitation of authigenic U-bearing phases (e.g., carbonates and phosphates) is a limiting factor for the U mobility. This result is very important for the mobility of U on Earth's surface (Riotte et al., 2003).

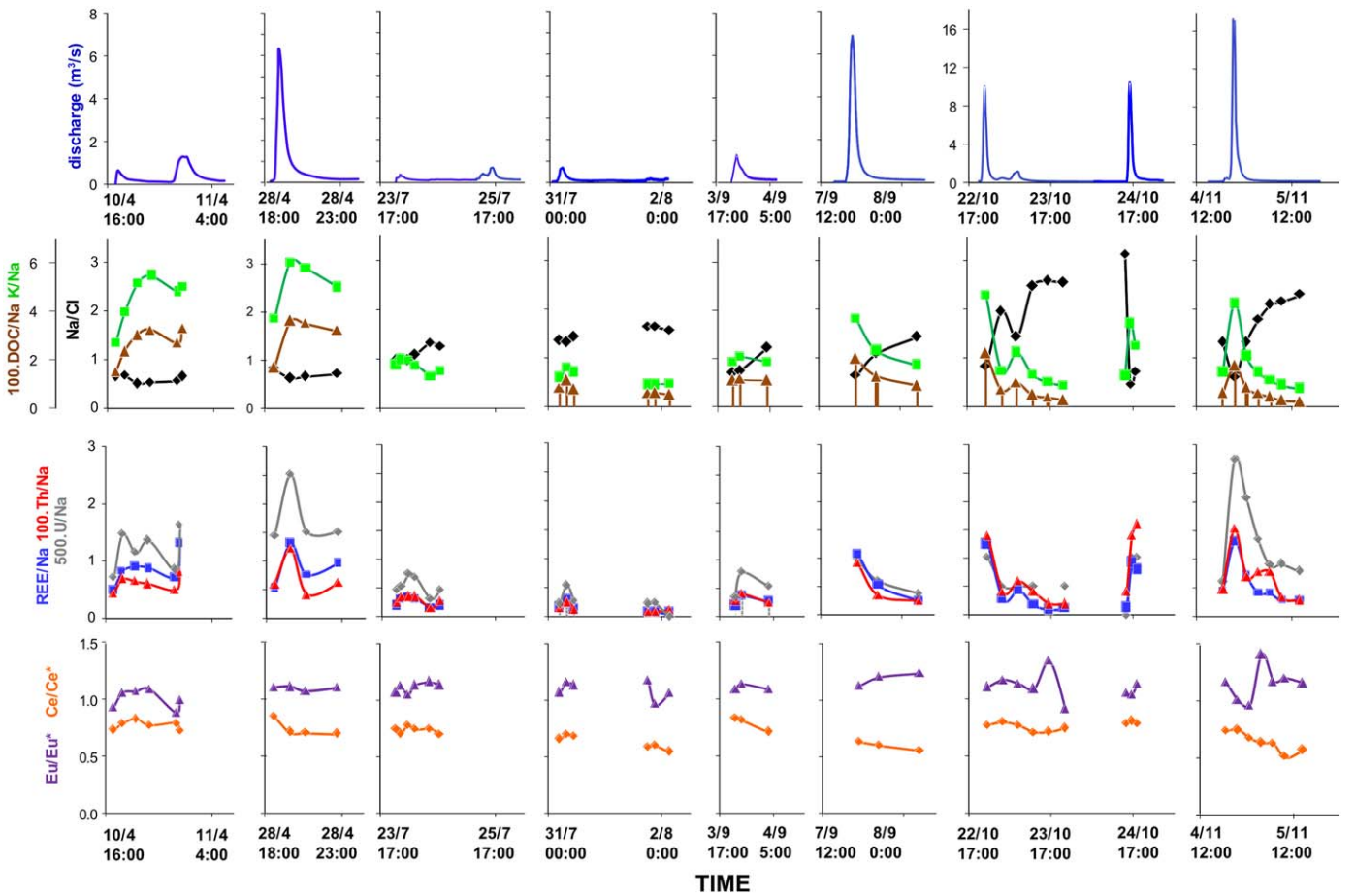

Figure 6. Time versus (i) discharge, (ii) Na/Cl molar ratio, and (iii) elemental Na-normalized molar ratio (REE, U, Th, DOC, and K) for sampled flood events along the water year 2005.

5.3. Solute/Colloidal Exports by the Stream

Annually, the water flowing into the intermittent Mule Hole CZO stream (94 ± 19 mm/yr) originates mainly from the overland flow on ferralsol (56%) and vertisol (31%) and, to a lesser extent, from ferralsol seepage (13%; i.e., pore water percolating through the soil horizons) during recession periods where vertisol being mostly impervious (Riotte et al., 2014a). Subsequently, the stream mainly exports solutes that were flushed from both forest floor processes and canopy interactions. Only exception is that the negligible amount of sodium cycling through vegetation (Riotte et al., 2014a, 2014b).

In order to get a better insight into the sources of soluble REE, Th, and U during the Mule Hole CZO flood events along the hydrological years, we plotted hourly fluctuations of Na-normalized molar ratios (REE, U, Th, K, and DOC) for selected flood events along the water year 2005. The samples without any influence of forest fire are mostly collected (Figure 6). Chemical weathering of primary silicates is appraised using Na as proxy with the Na/Cl molar ratio (see Riotte et al., 2014a). When the stream Na/Cl exceeds the rain Na/Cl ratio (0.85), a fraction of Na will be derived from the dissolution of Na-plagioclase in the soil layers.

The transfers of REE are driven by organic ligand chelation. Looking at the flood event scale permits us to better understand the origin of the elements, for example, REE, Th, U, DOC, and K are leached during the maximum peak discharge while Na is mostly released during the recession periods, confirming that REE, Th, U exported from the stream do not result from current weathering of primary silicates or authigenic phases. The solute contributions of the first floods of 2005 (Figure 6) are mostly due to interactions of rain, dust and canopy released products, while the contribution of forest floor and soil seepage is more significant in the last floods of the year (Figure 6). REE and Th are more affected by canopy interactions along with DOC, while U is less impacted. The release of HFSE in the stream waters is thus governed by reservoir contributions in varying time and space, which cannot be directly appraised only in property-property graphs.

6. Conclusion

The integrated study of the REY-Th-U solute reservoirs and vegetation cycles in the Mule Hole CZO allows us to draw the following hints:

1. The elemental input to the ground surface is controlled by canopy interactions and forest floor processes. The contribution of soluble REY due to the dissolution of dust deposits significantly takes place during the monsoon interseason and exceeds the REY brought by the vegetation cycling.
2. The vegetation cycling has a strong influence on the DOC concentration of the solutions that flow on the ground surface, and therefore, enhances the ability to chelate REY-Th-U. The resulting solute input to the soil is then enriched in elements coming from vegetation recycling (leave exudation, litter decay) and by dissolution of atmospheric dusts.
3. On a contemporary basis, the solute budget of REY-Th-U in the soil is maintained by the above ground fluxes, which make elements available for plant uptake.
4. The U leaching is much more significant in groundwater (high) than in the soil cover (low), indicating that primary U-beaing phases are currently weathered in the deepest part of the weathering cover.
5. At the weathering front, the plagioclase weathering is well traced by the positive Eu-anomaly in groundwater.
6. The stream mainly fed by overland flow water enhances the export of HFSE out of the system. The organic ligand chelation may considerably enhance the transfer of REE and Th but is less for U. The export of these elements is clearly dissociated from the primary silicate weathering.

Acknowledgments

The Mule Hole basin is part of the SNO-BVET project (Système National d'Observation-Bassin Versant Expérimentaux Tropicaux, http://bvet.omp.obs-mip.fr/index.php/eng/) belonging to the French "Network of Drainage Basins" (Réseau des Bassins Versants, RBV; http://rnbv.ipgp.fr/) and Infrastructure de Recherche OZCAR (Observatoire de la Zone Critique: Applications et Recherches). The Environmental Observatory BVET is supported by Institut de Recherche pour le Développement (IRD), Centre National de la Recherche Scientifique (Institut National des Sciences de l'Univers; CNRS/INSU) and Toulouse University. Our project has been benefited from funding from IRD and INSU/CNRS through the French program EC2CO (Ecosphère Continentale et Côtière) and ACI-Eau. We thank the Karnataka Forest Department and the staff of the Bandipur National Park for all the facilities and support they provided. The authors are thankful to both anonymous reviewers and to the Associate Editor whose comments considerably improved the quality of the manuscript.

References

Aubert, D., Le Roux, G., Krachler, M., Cheburkin, A., Kober, B., Shotyk, W., & Stille, P. (2006). Origin and fluxes of atmospheric REE entering an ombrotrophic peat bog in Black Forest (SW Germany): Evidence from snow, lichens and mosses. *Geochimica et Cosmochimica Acta*, *70*(11), 2815–2826. https://doi.org/10.1016/j.gca.2006.02.020

Aubert, D., Stille, P., Probst, A., Gauthier-Lafaye, F., Pourcelot, L., & Del Nero, M. (2002). Characterization and migration of atmospheric REE in soils and surface waters. *Geochimica et Cosmochimica Acta*, *66*(19), 3339–3350. https://doi.org/10.1016/S0016-7037(02)00913-4

Balestrini, R., Arisci, S., Brizzio, M. C., Mosello, R., Rogora, M., & Tagliaferri, A. (2007). Dry deposition of particles and canopy exchange: Comparison of wet, bulk and throughfall deposition at five forest sites in Italy. *Atmospheric Environment*, *41*, 745–756.

Barbiéro, L., Parate, H. R., Descloitres, M., Bost, A., Furian, S., Mohan Kumar, M. S., . . . Braun, J.-J. (2007). Using a structural approach to identify relationships between soil and erosion in a non-anthropic forested area, South India. *Catena*, *70*, 313–329.

Bhat, S., Jacobs, J. M., & Bryant, M. L. (2011). The chemical composition of rainfall and throughfall in five forest communities: A case study in Fort Benning, Georgia. *Water Air Soil Pollution*, *218*, 323–332.
Braun, J.-J., Descloitres, M., Riotte, J., Fleury, S., Barbiéro, L., Boeglin, J.-L., . . . Dupré, B. (2009). Regolith mass balance inferred from combined mineralogical, geochemical and geophysical studies: Mule Hole gneissic watershed, South India. *Geochimica et Cosmochimica Acta*, *73*(4), 935–961. https://doi.org/10.1016/j.gca.2008.11.013
Braun, J.-J., Pagel, M., Herbillon, A., & Rosin, C. (1993). Mobilization and redistribution of REEs and thorium in a syenitic lateritic profile: A mass balance study. *Geochimica et Cosmochimica Acta*, *57*(18), 4419–4434. https://doi.org/10.1016/0016-7037(93)90492-F
Braun, J.-J., Viers, J., Dupre, B., Polve, M., Ndam, J., & Muller, J.-P. (1998). Solid/liquid REE fractionation in the lateritic system of goyoum, East Cameroon: The implication for the present dynamics of the soil covers of the humid tropical regions. *Geochimica et Cosmochimica Acta*, *62*(2), 273–299.
Brimhall, G. H., Lewis, C. J., Ague, J. J., Dietrich, W. E., Hampel, J., Teague, T., & Rix, P. (1988). Metal enrichment in bauxites by deposition of chemically mature aeolian dust. *Nature*, *333*(6176), 819–824.
Brioschi, L., Steinmann, M., Lucot, E., Pierret, M. C., Stille, P., Prunier, J., & Badot, P. M. (2013). Transfer of rare earth elements (REE) from natural soil to plant systems: Implications for the environmental availability of anthropogenic REE. *Plant and Soil*, *366*(1), 143–163.
Bruijnzeel, L. A. (1989). Mineral nutrients in tropical forest and savannah ecosystems. In J. Proctor (Ed.), *Nutrient cycling in moist tropical forests: The hydrological framework* (pp. 383–415). Oxford, UK: Blackwell Scientific.
Bruijnzeel, L. A. (1990). *Hydrology of moist tropical forests and effects of conversion: A state of knowledge review—International Hydrological Programme-Humid Tropics Programme* (224 pp.). Paris, France: UNESCO.
Carlyle-Moses, D. E., Flores Laureano, J. S., & Price, A. G. (2004). Throughfall and throughfall spatial variability in Madrean oak forest communities of northeastern Mexico. *Journal of Hydrology*, *297*, 124–135.
Chabaux, F., Riotte, J., & Dequincey, O. (2003). U-Th-Ra fractionation during weathering and river transport. In B. Bourdon, G. M. Henderson, C. C. Lundstrom, & S. P. Turner (Eds.), *Uranium-series geochemistry* (pp. 533–576). Washington, DC: Geochemical Society-Mineralogical Society of America.
Davranche, M., Grybos, M., Gruau, G., Pédrot, M., Dia, A., & Marsac, R. (2011). Rare earth element patterns: A tool for identifying trace metal sources during wetland soil reduction. *Chemical Geology*, *284*(1–2), 127–137.
Derry, L. A., & Chadwick, O. A. (2007). Contributions from Earth's atmosphere to soil. *Elements*, *3*, 333–338.
Duff, M. C., Coughlin, J. U., & Hunter, D. B. (2002). Uranium co-precipitation with iron oxide minerals. *Geochimica et Cosmochimica Acta*, *66*(20), 3533–3547.
Dupré, B., Viers, J., Dandurand, J. L., Polvé, M., Bénezeth, P., Vervier, P., & Braun, J. J. (1999). Major and trace elements associated with colloids in organic-rich river waters ultrafiltration of natural and spiked solutions. *Chemical Geology*, *160*, 63–80.
Ferrat, M., Weiss, D. J., Strekopytov, S., Dong, S., Chen, H., Najorka, J., . . . Sinha, R. (2011). Improved provenance tracing of Asian dust sources using rare earth elements and selected trace elements for palaeomonsoon studies on the eastern Tibetan Plateau. *Geochimica et Cosmochimica Acta*, *75*(21), 6374–6399.
Ferrier, K. L., Kirchner, J. W., & Finkel, R. C. (2011). Estimating millennial-scale rates of dust incorporation into eroding hillslope regolith using cosmogenic nuclides and immobile weathering tracers. *Journal of Geophysical Research*, *116*, F03022. https://doi.org/10.1029/2011JF001991
Gandois, L., Agnan, Y., Leblond, S., Séjalon-Delmas, N., Le Roux, G., & Probst, A. (2014). Use of geochemical signatures, including rare earth elements, in mosses and lichens to assess spatial integration and the influence of forest environment. *Atmospheric Environment*, *95*, 96–104.
Gandois, L., Tipping, E., Dumat, C., & Probst, A. (2010). Canopy influence on trace metal atmospheric inputs on forest ecosystems: Speciation in throughfall. *Atmospheric Environment*, *44*, 824–833.
Goswami, V., Singh, S. K., & Bhushan, R. (2014). Impact of water mass mixing and dust deposition on Nd concentration and εNd of the Arabian Sea water column. *Geochimica et Cosmochimica Acta*, *145*, 30–49.
Gruau, G., Dia, A., Olivié-Lauquet, G., Davranche, M., & Pinay, G. (2004). Controls on the distribution of rare earth elements in shallow groundwaters. *Water Research*, *38*(16), 3576–3586. https://doi.org/10.1016/j.watres.2004.04.056
Grybos, M., Davranche, M., Gruau, G., & Petitjean, P. (2007). Is trace metal release in wetland soils controlled by organic matter mobility or Fe-oxyhydroxides reduction? *Journal of Colloid and Interface Science*, *314*(2), 490–501. https://doi.org/10.1016/j.jcis.2007.04.062
Gueniot, B., Munierlamy, C., & Berthelin, J. (1988a). Geochemical behavior of uranium in soils. 1. Influence of pedogenetic processes on the distribution of uranium in aerated soils. *Journal of Geochemical Exploration*, *31*(1), 21–37. https://doi.org/10.1016/0375-6742(88)90035-0
Gueniot, B., Munierlamy, C., & Berthelin, J. (1988b). Geochemical behavior of uranium in soils. 2. Distribution of uranium in hydromorphic soils and soil sequences—Applications for surficial prospecting. *Journal of Geochemical Exploration*, *31*(1), 39–55. https://doi.org/10.1016/0375-6742(88)90036-2
Jerden, J. L., Jr., Sinha, A. K., & Zelazny, L. (2003). Natural immobilization of uranium by phosphate mineralization in an oxidizing saprolite–soil profile: Chemical weathering of the Coles Hill uranium deposit, Virginia. *Chemical Geology*, *199*(1–2), 129–157.
Lacaux, J. P., Loemba-Ndembi, J., Lefeivre, B., Cros, B., & Delmas, R. (1992). Biogenic emissions and biomass burning influences on the chemistry of the fogwater and stratiform precipitations in the African equatorial forest. *Atmospheric Environment*, *26A*, 541–551.
Langmuir, D., & Herman, J. S. (1980). The mobility of thorium in natural waters at low temperatures. *Geochimica et Cosmochimica Acta*, *44*(11), 1753–1766.
Laveuf, C., & Cornu, S. (2009). A review on the potentiality of Rare Earth Elements to trace pedogenetic processes. *Geoderma*, *154*(1–2), 1–12.
Laveuf, C., Cornu, S., & Juillot, F. (2008). Rare earth elements as tracers of pedogenetic processes. *Comptes Rendus Geoscience*, *340*(8), 523–532. https://doi.org/10.1016/j.crte.2008.07.001
Lin, H. (2010). Earth's Critical Zone and hydropedology: Concepts, characteristics and advances. *Hydrological Earth System Science*, *14*, 25–45.
Lindberg, S. E., Lovett, G. M., Richter, D. D., & Johnson, D. W. (1986). Atmospheric deposition and canopy interactions of major ions in a forest. *Science*, *231*, 141–145.
Lovett, G. M., & Lindberg, S. E. (1984). Dry deposition and canopy exchange in a mixed oak forest as determined by analysis of throughfall. *Journal of Applied Ecology*, *21*, 1013–1027.
Marechal, J.-C., Varma, M. R. R., Riotte, J., Vouillamoz, J.-M., Mohan Kumar, M. S., Ruiz, L., . . . Braun, J.-J. (2009). Indirect and direct recharges in a tropical forested watershed: Mule Hole, India. *Journal of Hydrology*, *364*(3–4), 272–284. https://doi.org/10.1016/j.jhydrol.2008.11.006
Maréchal, J. C., Riotte, J., Lagane, C., Subramanian, S., Kumar, C., Ruiz, L., . . . Braun, J. (2011). Deep groundwater flow as the main pathway for chemical outputs in a small headwater watershed. *Applied Geochemistry*, *26*, S94–S96.
Naqvi, S. M., & Rogers, J. W. (1987). *Precambrian geology of India* (223 pp.). New York, NY: Oxford University Press.
Potter, C. S., Ragsdale, H. L., & Swank, W. T. (1991). Atmospheric deposition and foliar leaching in a regenerating southern Appalachian forest canopy. *Journal of Ecology*, *79*, 97–115.

Pourret, O., Davranche, M., Gruau, G., & Dia, A. (2007a). Organic complexation of rare earth elements in natural waters: Evaluating model calculations from ultrafiltration data. *Geochimica et Cosmochimica Acta*, *71*(11), 2718–2735. https://doi.org/10.1016/j.gca.2007.04.001

Pourret, O., Davranche, M., Gruau, G., & Dia, A. (2007b). Rare earth elements complexation with humic acid. *Chemical Geology*, *243*(1–2), 128–141. https://doi.org/10.1016/j.chemgeo.2007.05.018

Ribera, D., Labrot, F., Tisnerat, G., & Narbonne, J. F. (1996). Uranium in the environment: Occurrence, transfer, and biological effects. *Reviews of Environmental Contamination and Toxicology*, *146*, 53–89.

Riotte, J., Chabaux, F., Benedetti, M., Dia, A., Gerard, M., Boulegue, J., & Etame, J. (2003). Uranium colloidal transport and origin of the ^{234}U-^{238}U fractionation in surface waters: New insights from Mount Cameroon. *Chemical Geology*, *202*(3–4), 365–381.

Riotte, J., Maréchal, J. C., Audry, S., Kumar, C., Bedimo, J. P. B., Ruiz, L., . . . Braun, J. J. (2014a). Vegetation impact on stream chemical fluxes: Mule Hole watershed (South India). *Geochimica et Cosmochimica Acta*, *145*, 116–138. https://doi.org/10.1016/j.gca.2014.09.015

Riotte, J., Ruiz, L., Audry, S., Sekhar, M., Mohan Kumar, M. S., Siva Soumya, B., & Braun, J. J. (2014b). Impact of vegetation and decennial rainfall fluctuations on the weathering fluxes exported from a dry tropical forest (Mule Hole). *Procedia Earth and Planetary Science*, *10*, 34–37. https://doi.org/10.1016/j.proeps.2014.08.007

Ruiz, L., Varma, M. R. R., Kumar, M. S. M., Sekhar, M., Maréchal, J.-C., Descloitres, M., . . . Braun, J.-J. (2010). Water balance modelling in a tropical watershed under deciduous forest (Mule Hole, India): Regolith matric storage buffers the groundwater recharge process. *Journal of Hydrology*, *380*(3–4), 460–472. https://doi.org/10.1016/j.jhydrol.2009.11.020

Shadakshara Swamy, N., Jayananda, M., & Janardhan, A. S. (1995). Geochemistry of Gundlupet gneisses, Southern Karnataka: A 2.5 Ga old reworked sialic crust. In M. Yoshida, M. Santosh, & A. T. Rao (Eds.), *India as a fragment of East Gondwana* (pp. 87–97). Gondwana Research Group.

Sheppard, S. C., & Evenden, W. G. (1988). Critical compilation and review of plant/soil concentration ratios for uranium, thorium and lead. *Journal of Environmental Radioactivity*, *8*(3), 255–285. https://doi.org/10.1016/0265-931X(88)90051-3

Soumya B. S., Sekhar, M., Riotte, J., & Braun, J.-J. (2009). Non-linear regression model for spatial variation in precipitation chemistry for South India. *Atmospheric Environment*, *43*, 1147–1152.

Steinmann, M., & Stille, P. (2008). Controls on transport and fractionation of the rare earth elements in stream water of a mixed basaltic-granitic catchment basin (Massif Central, France). *Chemical Geology*, *254*(1–2), 1–18. https://doi.org/10.1016/j.chemgeo.2008.04.004

Stille, P., Pierret, M. C., Steinmann, M., Chabaux, F., Boutin, R., Aubert, D., . . . Morvan, G. (2009). Impact of atmospheric deposition, biogeochemical cycling and water–mineral interaction on REE fractionation in acidic surface soils and soil water (the Strengbach case). *Chemical Geology*, *264*(1–4), 173–186. https://doi.org/10.1016/j.chemgeo.2009.03.005

Stille, P., Steinmann, M., Pierret, M. C., Gauthier-Lafaye, F., Chabaux, F., Viville, D., . . . Aubert, D. (2006). The impact of vegetation on REE fractionation in stream waters of a small forested catchment (the Strengbach case). *Geochimica et Cosmochimica Acta*, *70*(13), 3217–3230. https://doi.org/10.1016/j.gca.2006.04.028

Takahashi, Y., Châtellier, X., Hattori, K. H., Kato, K., & Fortin, D. (2005). Adsorption of rare earth elements onto bacterial cell walls and its implication for REE sorption onto natural microbial mats. *Chemical Geology*, *219*(1–4), 53–67. https://doi.org/10.1016/j.chemgeo.2005.02.009

Taunton, A. E., Welch, S. A., & Banfield, J. F. (2000). Microbial controls on phosphate and lanthanide distributions during granite weathering and soil formation. *Chemical Geology*, *169*(3–4), 371–382. https://doi.org/10.1016/S0009-2541(00)00215-1

Tyler, G. (2004). Rare earth elements in soil and plant systems—A review. *Plant and Soil*, *267*(1), 191–206. https://doi.org/10.1007/s11104-005-4888-2

Vázquez-Ortega, A., Perdrial, J., Harpold, A., Zapata-Ríos, X., Rasmussen, C., McIntosh, J., . . . Chorover, J. (2015). Rare earth elements as reactive tracers of biogeochemical weathering in forested rhyolitic terrain. *Chemical Geology*, *391*, 19–32. https://doi.org/10.1016/j.chemgeo.2014.10.016

Viers, J., Dupre, B., Polve, M., Schott, J., Dandurand, J. L., & Braun, J. J. (1997). Chemical weathering in the drainage basin of a tropical watershed (Nsimi-Zoetele site, Cameroon): Comparison between organic poor and organic rich waters. *Chemical Geology*, *140*, 181–206.

Vinoj, V., Rasch, P. J., Wang, H., Yoon, J.-H., Ma, P.-L., Landu, K., & Singh, B. (2014). Short-term modulation of Indian summer monsoon rainfall by West Asian dust. *Nature Geoscience*, *7*(4), 308–313.

Violette, A., Goddéris, Y., Maréchal, J.-C., Riotte, J., Oliva, P., Kumar, M. S. M., . . . Braun, J.-J. (2010a). Modelling the chemical weathering fluxes at the watershed scale in the Tropics (Mule Hole, South India): Relative contribution of the smectite/kaolinite assemblage versus primary minerals. *Chemical Geology*, *277*(1–2), 42–60. https://doi.org/10.1016/j.chemgeo.2010.07.009

Violette, A., Riotte, J., Braun, J.-J., Oliva, P., Marechal, J.-C., Sekhar, M., . . . Dupre, B. (2010b). Formation and preservation of pedogenic carbonates in South India, links with paleo-monsoon and pedological conditions: Clues from Sr isotopes, U–Th series and REEs. *Geochimica et Cosmochimica Acta*, *74*(24), 7059–7085. https://doi.org/10.1016/j.gca.2010.09.006

Yadav, S., & Rajamani, V. (2004). Geochemistry of aerosols of northwestern part of India adjoining the Thar Desert. *Geochimica et Cosmochimica Acta*, *68*(9), 1975–1988. https://doi.org/10.1016/j.gca.2003.10.032